

# Development of a Rabbit Pleural Cancer Model by Using VX2 Tumors

Kelly A. Kreuter,<sup>1</sup> Naglaa El-Abbadi,<sup>1</sup> Alia Shbeeb,<sup>1</sup> Lillian Tseng,<sup>1</sup> Sari Brenner Mahon,<sup>1</sup> Navneet Narula,<sup>3</sup> Tanya Burney,<sup>1</sup> Henri Colt,<sup>2</sup> and Matthew Brenner<sup>1,2,\*</sup>

Primary and secondary pleural cancer remains an important clinical problem, with research progress limited by the lack of a suitable moderate- to large-sized (3 to 4 kg) animal model of pleural cancer. Many potential pleura-based imaging and treatment modalities cannot be investigated sufficiently by using currently available small murine animal models because their pleural space is not comparable to that of humans and therefore does not allow for the use of standard thoroscopic techniques. Here we describe the development of a reproducible model of pleural malignancy in moderate-sized immunocompetent rabbits. Under thoroscopic guidance,  $9\text{--}15 \times 10^6$  VX2 carcinoma cells were inoculated into the pleural space of 3 to 4 kg New Zealand white rabbits that had undergone gentle pleural abrasion. Malignant tumor involvement developed on the visceral and parietal pleural surfaces in an average of 2 to 4 wk. This novel pleural tumor model induction method likely will facilitate a broad range of investigations of pleural cancer diagnostics and therapeutics.

Pleural malignancy remains one of the most refractory problems in the treatment of patients with cancer. The success of primary pleural mesothelioma treatment remains very limited, with median survival rates reported in the range of less than 1 to 2 y.<sup>4,15,19</sup> Malignant pleural effusions resulting from lung cancer define stage IIIB disease and unresectability.<sup>10,12,17</sup> In addition, metastatic pleural disease from other cancers is associated with serious morbidity and mortality consequences.<sup>1,8,11</sup> Despite the importance of primary and secondary pleural malignancies, progress in treatment advances has been limited in part by lack of suitable moderate- to large-sized (3 to 4 kg) pleural cancer animal models for research.

The pleural space is a large and complex anatomic region within the thorax adjacent to vital structures; the anatomy of the pleural space presents substantial access and dosimetry challenges for cancer diagnostics as well as therapeutics. Because standard human medical equipment will not fit into the murine pleural space, many potential pleura-based imaging and treatment modalities cannot be adequately investigated by using currently available small murine pleural malignancy models.<sup>13,16,18</sup> Moderate-sized, immunocompetent animal models of pleural malignancy are needed to address these issues because the pleural space of these animals can accommodate instruments designed for human use in pediatric care. Compared with mice and rats, New Zealand white rabbits that weigh 3 to 4 kg have a pleural space that is more analogous to that found in humans. This similarity makes the model more practical for studying diagnostic techniques and emerging therapies.

In this report, we describe the development of a consistent, reproducible model of pleural carcinoma in moderate-sized (3 to 4 kg) immunocompetent rabbits. This model likely will be useful in developing diagnostic and treatment methodologies, such as high-resolution thoroscopic optical technologies, surgical procedures, and therapeutics, such as photodynamic therapy, that cannot be investigated sufficiently in existing smaller animal models. We also describe various methods of VX2-induced tumor cell maintenance and propagation by parenchymal, intravenous, and intramuscular implantation.

## Materials and Methods

The procedures involving live vertebrate animals were reviewed and approved by the University of California–Irvine Institutional Animal Care and Use Committee. The institutional animal care and use program is covered by Assurance of Compliance with PHS Policy #3416-01 and is fully AAALAC-accredited.

**Animal preparation.** Pathogen-free male New Zealand white rabbits (*Oryctolagus cuniculus*; Western Oregon Rabbit Supply, Philomath, OR) weighing 3 to 4 kg were used in this study. They were housed in the vivarium at the University of California–Irvine. The animals were anesthetized with a 2:1 ratio of ketamine HCl (100 mg/ml; Ketaset, Fort Dodge Animal Health, Fort Dodge, IA) and xylazine (20 mg/ml; Phoenix Pharmaceutical, St Joseph, MO) at a dose of 0.75 ml/kg IM in the hind leg. After injection, a 23-gauge, 1-in. catheter was placed in a marginal ear vein for administration of IV anesthesia. The depth of anesthesia was evaluated by monitoring the physical reflexes of the animal (no voluntary head, limb, or eye movements) and pulse rate. Maintenance anesthetic dosed at 0.3 ml of a 1:1 mixture of ketamine and xylazine (ketamine, 100 mg/ml; xylazine, 20 mg/ml) was administered accordingly. A dose of analgesic (0.1 to 0.5 mg/kg SC; Torbutrol, Torbugesia-SA, Fort Dodge Animal Health,

Received: 18 Feb 2007. Revision requested: 12 March 2007. Accepted: 24 May 2007.

<sup>1</sup>Beckman Laser Institute, University of California Irvine, Irvine, CA; <sup>2</sup>Pulmonary and Critical Care Division, <sup>3</sup>Pathology Division, UC Irvine Medical Center, Orange, CA

\*Corresponding author. Email: mbrenner@uci.edu

Fort Dodge, IA) was given prior to intubation. The animals were intubated with a 3.0 French cuffed endotracheal tube and were ventilated (dual-phase control respirator, model 32A4BEPM-5R, Harvard Apparatus, Chicago, IL) at a rate of 32 respirations/min, tidal volume of 50 cc, and inspired O<sub>2</sub> fraction of 100%.

Animals undergoing surgical thoracoscopic implantation of tumor were prepared for surgery. The right side of the chest was shaved, and the rabbit was placed on the operating table with its shaved side up. The operative sites were scrubbed (Nolvasan Surgical Scrub, Fort Dodge Animal Health, Fort Dodge, IA) and then rinsed (Nolvasan Solution, Fort Dodge Animal Health, Fort Dodge, IA). The site then was draped with a 40 × 40 in. sterile drape.

**VX2 tumors.** This study uses VX2 tumors, which are classified as carcinomas and which were derived initially in 1940.<sup>6</sup> These tumors are considered to be a wholly anaplastic carcinoma whose keratinocytes never keratinize.<sup>3</sup> VX2 tumor cells grow rapidly in allogenic adult recipients and frequently metastasize to the lungs.<sup>5</sup> They are known for rapid growth and can be transplanted serially. These tumor cells can also be propagated in the thigh muscle.<sup>3,6</sup> The tumor used in this study was of rabbit origin and was isolated from rabbit skin warts produced by the Shope cottontail rabbit papillomavirus.<sup>14</sup>

**Preparation of primary tumor cells.** Rabbit lungs containing VX2 tumors were removed from euthanized animals and washed in 3 (20 min each) changes of PBS containing gentamicin sulfate (0.200 mg/ml; Fisher Scientific, Pittsburg, PA) and amphotericin B (0.0224 mg/ml; Sigma, St Louis, MO).<sup>10</sup> Tumors were excised from lung tissue, placed in a small amount of warm (37 °C) DMEM containing 10% fetal bovine serum (GIBCO cell culture, Invitrogen, Carlsbad, CA), and cut into approximately 1-mm pieces. Surplus tumor tissue was stored by suspension in DMEM containing 10% DMSO and freezing at -80°. The remaining tumor tissue was homogenized thoroughly in DMEM by using a Wheaton glass homogenizer, and the resultant cell suspension was transferred to 15-cc centrifuge tubes. Cells were centrifuged at 45 × g for 5 min and resuspended in red cell lysis buffer (8.3 g/l ammonium chloride in 0.01 Tris-HCl, pH 7.5) for 5 min. After centrifugation (45 × g, 5 min), cells were resuspended in PBS (without Ca<sup>2+</sup> or Mg<sup>2+</sup>) and counted by hemocytometer. The desired number of cells then was injected into New Zealand white rabbits by 1 of 3 possible routes (see section titled 'Tumor implantation models'). The remainder of the cell preparation was frozen for future use after centrifugation (45 × g, 5 min) and resuspension in DMEM with 10% DMSO. Vials containing 16–24 × 10<sup>6</sup> cells were frozen in liquid nitrogen.

**Preparation of frozen cells for injection.** In general, primary fresh tumor cells were preferred for implantation because of their consistent and rapid growth. However, frozen cells could be used, and in our study were used frequently because of the abundance of the stock supply. To prepare cells for injection after freezing, vials of cells were thawed in a 37 °C water bath, centrifuged as earlier, and resuspended either in PBS for injection or in DMEM for incubation or culture at 37 °C prior to injection.

**Preparation of cells from frozen lung tumors.** To prepare cells from frozen tissues, vials of tissues are defrosted in a 37 °C water bath, and prepared as above with homogenization, red cell lysis, and cell counting.

**Tumor implantation models. Pleural implantation of tumor.** After anesthesia induction and intubation of rabbits, a 4-mm thora-

scope was inserted into the 5th or 6th intercostal space at the mid-axillary line by using trocars. Under thoracoscopic visualization, a small section of the chest wall parietal pleura was abraded gently with the wooden end of a sterile cotton-tip applicator. This technique was used to abrade the tissue so that the cells could adhere. Mild to moderate abrasion was generated until the tissue turned from pinkish to red, and occasionally some bleeding was observed. An inoculum of VX2 tumor cells (9–15 × 10<sup>6</sup> cells in 0.1 to 0.5 ml of Hanks buffered saline solution) was injected into the right chest cavity adjacent to the abraded pleural surface by using a sterile syringe. Once the surgery was completed, the incisions were sewn with 0 silk, and epidermal glue (Nexaband, Abbott Laboratories, Abbott Park, IL) was placed over the incision site. Before the animals were allowed to recover from anesthesia, they were given enrofloxacin (0.7 ml of 22.7 mg/ml; Baytril, Bayer Animal Health, Shawnee Mission, KS) prophylactically to prevent infection. Because this was a relatively minor procedure and there was little risk of post-operative discomfort, animals were not given any analgesic at this time, unless they showed outward signs of distress.

At 21 d after implantation (or earlier if animals were dyspnic), a second thoracoscopy was performed. If tumor was found, the animals underwent immediate sternotomy and were euthanized for histologic characterization of the tumor and implantation site. If no tumor cells were detected, the thoracoscope was removed, the thoracotomy site was sutured close by using sterile technique, and the animals were allowed to recover from anesthesia. A repeat thoracoscopy was performed after another 2 wk (or when the animals showed signs of dyspnea); animals were euthanized at this point, regardless of whether tumor was detected.

**Parenchymal implantation of tumor.** By using the same thoracoscopic and visualization techniques described earlier, a moderate inoculum of VX2 tumor cells (9–15 × 10<sup>6</sup> cells in 0.1 to 0.5 ml of Hanks buffered saline solution) was injected into the right lower lobe of the lung. At 21 d after tumor implantation, a repeat thoracoscopy was done to determine the progress of tumor growth. If tumor was found, animals were euthanized, and tumor cells were harvested. If no tumor cells were detected, the animals were allowed to recover from anesthesia and were maintained until a repeat thoracoscopy was performed 2 wk later. At that point all animals were euthanized, regardless of whether tumor was detected.

**Hematogenous implantation of tumor.** After anesthesia induction, a moderate inoculum of 10–25 × 10<sup>6</sup> VX2 carcinoma cells was injected into the catheter, followed by a 2- to 3-ml heparin flush. At 21 d after injection, thoracoscopy was performed using the same techniques as described above. If tumor was found, animals were euthanized, and tumor cells were harvested. If no tumor cells were detected, the animals were allowed to recover from anesthesia and were maintained until a repeat thoracoscopy was performed 2 wk later. At that point, all animals were euthanized, regardless of whether tumor was detected.

**Intramuscular implantation of tumor.** By using a 3-ml syringe with a 23-gauge needle, VX2 tumor (9–15 × 10<sup>6</sup> cells in 0.1 to 0.5 ml of Hanks buffered saline solution) cells were injected into the right thigh muscle of the animals. At 21d after injection, the right thigh was palpated and compared with the left thigh muscle. If a palpable mass of greater than 2 cm was felt on gross exam at the site of the injection, the animal was euthanized. Tumor cells from the right thigh were removed by standard dissection and

harvested. If no palpable mass was detected, a second examination was performed after 2 wk or whenever the animals appeared ill. At that time, all remaining animals were euthanized and the tumor cells were harvested.

**Radiographic examination to supplement thoracoscopy.** Parenchymal, pleural, and IV tumor induction models were evaluated with respect to the use of high-resolution digital chest radiographic examination as a noninvasive approach to detecting tumors. At day 21 after tumor cell implantation and before the first exploratory thoracoscopy, animals were anesthetized for radiographic examination by IM injection of 3 cc of 2:1 ketamine:xylazine into the thigh. Digital images of the chest cavity were acquired by using a biplane system with a constant potential X-ray generator (Optimus M200, Philips Medical Systems, Shelton, CT), 23 × 17 × 13 cm CsI image intensifiers, focused grids (8:1 grid ratio, 36 lines/cm), and charge-coupled device cameras (Multicam MC-1134GN, TX Instruments, Dallas, TX). Adjustable apertures controlled the light intensity in front of the cameras. The video signals were linearly digitized to 512 × 480 × 8-bit precision by using 2 frame grabbers (Matrox Electronics Systems, Dorval, Quebec, Canada) and a Pentium IV computer. The images were acquired by using a large (1.2 mm nominal) focal spot in the 5-in. image intensifier mode. Rabbits were placed at the isocenter of the biplane system. Source-to-image distances were approximately 89 cm and 98 cm for the anteroposterior and lateral projections, respectively. Tube voltage (kVp), tube current, and exposure times were chosen automatically with an automatic exposure control. Typical voltages ranged from 48 to 57 kVp, depending on the size and orientation of the rabbits. The images were evaluated for detection of tumors. Regardless of the results of this imaging, animals were taken to the operating room for exploratory thoracoscopy as described earlier.

**Terminal surgery for tumor excision.** If the thoracoscopy revealed sufficient tumor growth, the animals were euthanized with 1 to 2 ml of Euthasol (350 mg pentobarbital sodium and 50 mg phenytoin sodium per ml, Virbac Animal Health, Fort Worth, TX) administered through the marginal ear vein, followed by 0.5 ml of heparin flush. Once the animals had died, a median sternotomy was performed. A 10-cm incision was made over the sternum. The sternum was divided with a cutting scissor and separated with a retractor, exposing the pleural and pericardial surfaces (Figure 1). The chest cavity was examined, and any areas showing malignancy were resected and saved for histologic processing and staining with hematoxylin and eosin.

**Immunohistochemical staining.** Tissue specimens were fixed in 10% formalin, embedded in paraffin, and cut into sections of 4 μm thickness. Tissues were deparaffinized and rehydrated in alcohol followed by treatment with retrieval solution (S1699, Dako, Carpinteria, CA) in a pressure cooker for 45 min. The remainder of the staining process was performed automatically (Autostainer Plus, Dako). After blocking of endogenous peroxidase activity with peroxidase blocking reagent (S2001, Dako), the sections were cooled to room temperature by incubating for 5 min in hot buffer then followed by wash buffer. Sections then were incubated for 30 min at room temperature with antibodies to the following antigens: AE1/AE3 (1:100; M3515, Dako), desmin (1:120; M0760, Dako), calretinin (1:200; M7245, Dako), SMA (1:100; M0851, Dako), vimentin (1:1000; M0725, Dako), myogenin (1:1000; M3559, Dako), Ki67 (1:1000; M7240, Dako), B72.3 (1:10; AM054-5M, Biogenex, San Ramon, CA), CAM5.2 (1:5; 349205, Becton Dickinson, San

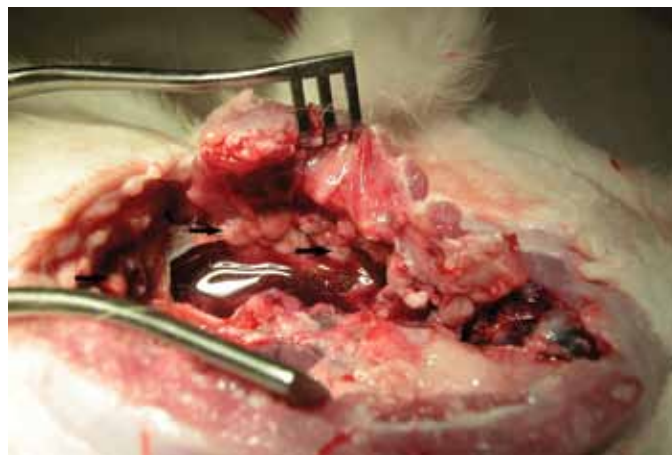


**Figure 1.** Rabbit 16 d after implantation of previously frozen cells onto the pleura. Extensive involvement of the parietal pleura is seen, along with a large pleural effusion. Black arrows indicate tumor nodules.

Jose, CA), CD15 (prediluted; PAB116, Ventana, Theson, AZ), and CEA (1:5; monoclonal, AM009-5M, Biogenex). For negative control, a slide was incubated with normal mouse IgG (1:200; x0931, Dako). After washing in PBS buffer, the sections were treated with biotinylated antimouse IgG (1:200; BA2000, Vector Laboratories, Burlingame, CA) followed by ABC-Elite standard kit (PK-6100, Vector Laboratories) for 30 min each at room temperature. Reaction product was visualized with DAB Plus (K3468, Dako). Sections were counterstained with hematoxylin and mounted in mounting medium (4111, Richard-Allan Scientific, Kalamazoo, MI).

## Results

**Pleural tumor inoculation.** Tumor cells were injected into the pleural space of 14 rabbits; 9 animals received previously frozen cells, whereas the remaining 5 received fresh tumor. Of the 9 that were injected with previously frozen cells, 7 successfully grew tumor over an average of 18 d until euthanized (Figure 1, Figure 2 A, B). All 5 of the rabbits that received fresh cells grew tumor over an average of 24 d; in 3 of the 5 rabbits, the tumor spread to the diaphragm.

Pleural tumor spread to, and frequently invaded, the chest wall parietal pleural surface, lung visceral pleural surface, ribs (Figure 2 C), and diaphragmatic surfaces (Figure 2 D) after an average of 18 d. In addition, 1 of the injected rabbits exhibited tumors on the pericardium (Figure 3).

**Radiography.** Of the 65 rabbits injected with tumor, only 10 underwent high-resolution digital chest radiographic examination because this section of the protocol was added late in the study. Of these 10 rabbits, cells had been injected into the pleural space of 4 animals, 1 rabbit had an IM injection, and 5 had IV tumor injections. All rabbits showed suspected lung nodules by radiography, and thoracoscopy confirmed these findings. The purpose of this addition to the study protocol was to assess whether radiography was sufficiently sensitive to detect malignancy, because this technology would provide a noninvasive way to monitor tumor growth. The chest radiographs were relatively insensitive for direct visualization of pleural tumors in the rabbit model. However, they were able to reveal pleural effusions, which were indicative of underlying pleural malignancy in this model.



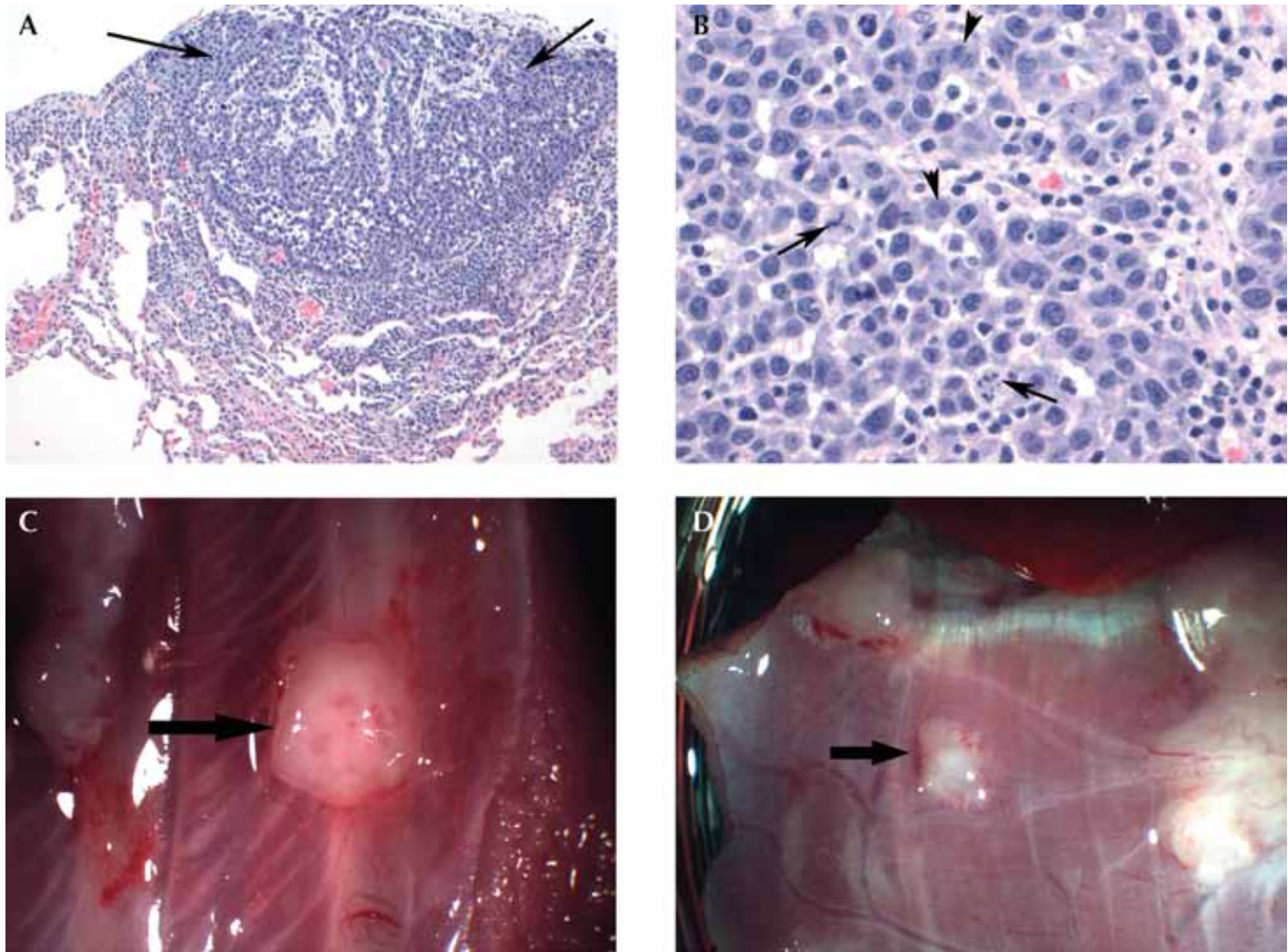


**Figure 2.** (A) The image shows proliferation of epithelial cells (arrows) in a tubulopapillary pattern, forming a nodule on the surface of the visceral pleura. There is minimal invasion into the underlying pleura, and no invasion of the lung parenchyma is seen. Hematoxylin and eosin stain; magnification,  $\times 100$ . (B) This higher magnification of the tumor shows round to polygonal tumor cells with a moderate amount of eosinophilic cytoplasm. Glandular formation (arrowheads) as well as atypical mitoses (arrows) are seen. Hematoxylin and eosin stain; magnification,  $\times 400$ . (C) Tumor on a rib 12 d after pleural implantation of previously frozen tumor cells. (D) Diaphragmatic tumor 12 d after pleural implantation of previously frozen cells.

**Intramuscular, intravenous, and lung parenchymal inoculation of tumor cells.** In addition to the pleural inoculations that were the focus of this study, tumor could be passed from animal to animal by intramuscular injection, intravenous injection (modified from methods previously described by other investigators),<sup>2</sup> or injection into the pulmonary parenchyma (Figure 4). The additional injection sites were added to increase the tumor cell source supply. These injection methods resulted in different presentations. Intramuscular injection resulted in an initially localized thigh muscular tumor mass that eventually spread to the lung parenchyma. The intravenous and direct parenchymal injections both resulted in lung parenchymal tumors. All 3 of the rabbits that received parenchymal injections successfully grew tumor. In addition, 29 of the 33 were injected intravenously successfully grew tumor, and 13 of the 15 rabbits implanted intramuscularly grew tumor.

**Pathologic characterization.** Pathologic examination of VX2 pleural tumors produced in this study revealed characteristics

typical of carcinomas. Pleural tumors obtained by thoracoscopic implantation ranged from small clusters of malignant cells that infiltrated the chest wall, diaphragm, and underlying lung to macroscopically visible nodules as large as 3 mm. The tumors were predominantly pleura-based, both visceral and parietal. Histologically, the tumor consisted of epithelioid cells arranged in sheets, solid nests, and glandular patterns. The cells had a high nuclear:cytoplasmic ratio, with eosinophilic cytoplasm. The nuclei had small to inconspicuous nucleoli and were very mitotically active, with mitotic counts as high as 5 to 6 per high-power field. Numerous atypical mitoses are present. The clusters of epithelioid cells are separated by a desmoplastic spindle cell stroma. Immunohistochemical stains were performed to further characterize these malignant cells. The cells were strongly positive for keratin AE1/AE3 (Figure 5 A) and showed diffuse and strong nuclear staining for Ki67 (Figure 5 B), a marker of cell proliferation. Scattered cells were positive for vimentin (Figure 5 C). The tumor cells were negative (as compared with positive rabbit con-

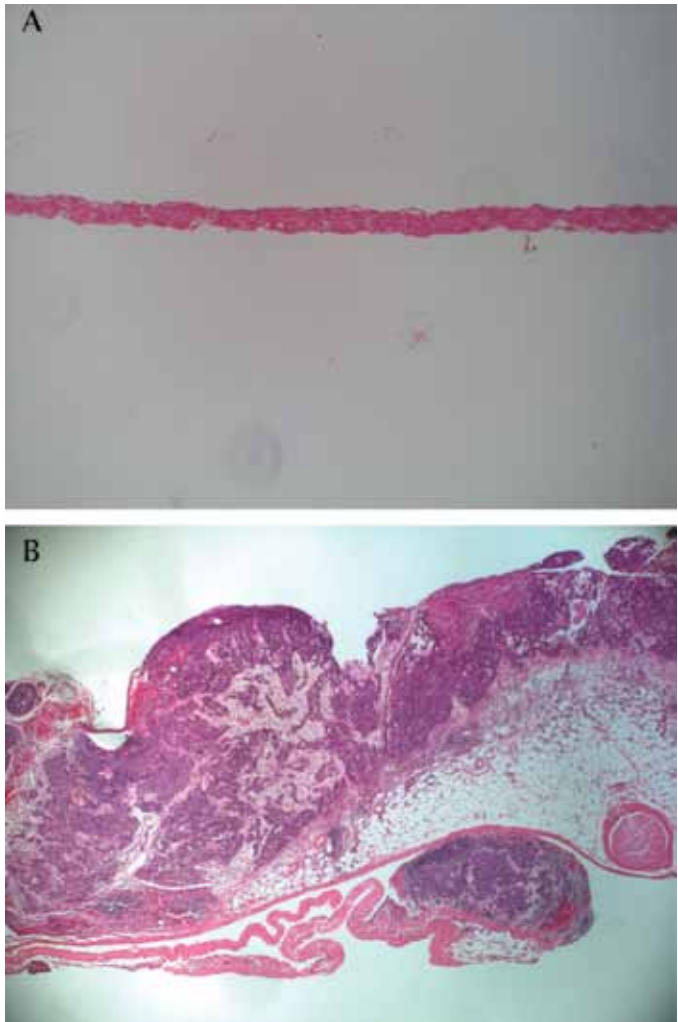


**Figure 3.** (A) Normal rabbit pericardium. Magnification,  $\times 100$ . (B) Pericardial tumor 13 d after pleural implantation of previously frozen cells. Hematoxylin and eosin stain; magnification,  $\times 40$ .

trols) for low-molecular-weight cytokeratin (Cam5.2), markers of adenocarcinoma (CD15 and B72.3), and muscle markers (desmin, smooth muscle actin, myogenin).

### Discussion

This study demonstrated the successful development of a consistent and reproducible pleural cancer model in moderate-sized immunocompetent animals. Such models are needed in several areas of cancer detection and treatment investigation. The tumor line used in these studies originated from cultured rabbit VX2 tumor. However, the morphologic characteristics of cells from recent passages have drifted such that they are now suggestive of well to moderately differentiated epithelioid malignancy similar in appearance to primary mesothelioma. In addition, the immunohistochemistry of the current tumor is consistent with mesothelioma, as multiple markers for adenocarcinoma are negative. The clinical presentation shares many characteristics of primary and secondary pleural cancers in patients, including development of pleural effusions and tumor involvement of the visceral and parietal pleura as well as the diaphragm. In some rabbits, clinical

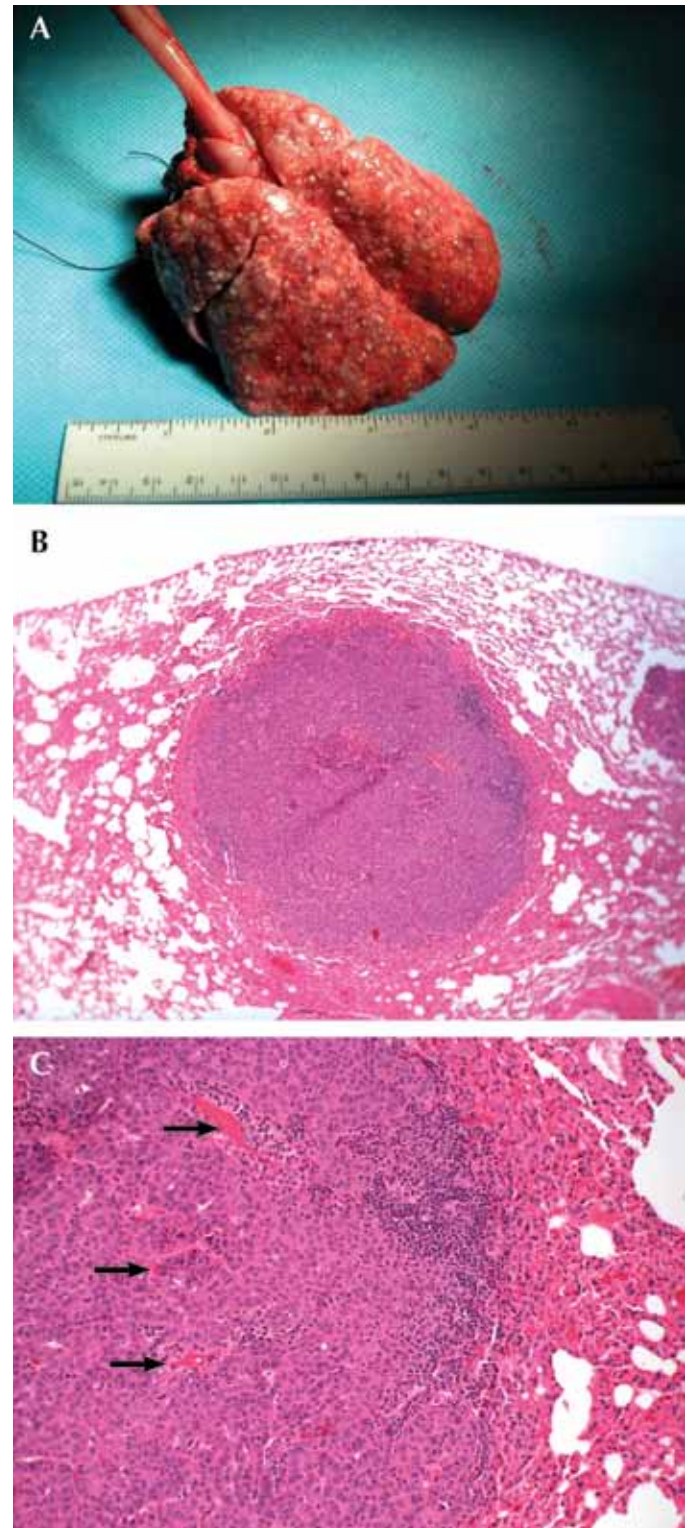


**Figure 4.** (A) Hematogenous spread of VX2 tumors to the lungs. Note the cobblestone appearance of the normally smooth lungs. (B) Tumor that localized to the lung 20 d after IV implantation with previously frozen cells. Hematoxylin and eosin; magnification,  $\times 40$ . (C) High magnification of the lung tumor. Hematoxylin and eosin; magnification,  $\times 100$ . Arrows point to notable vascularization.



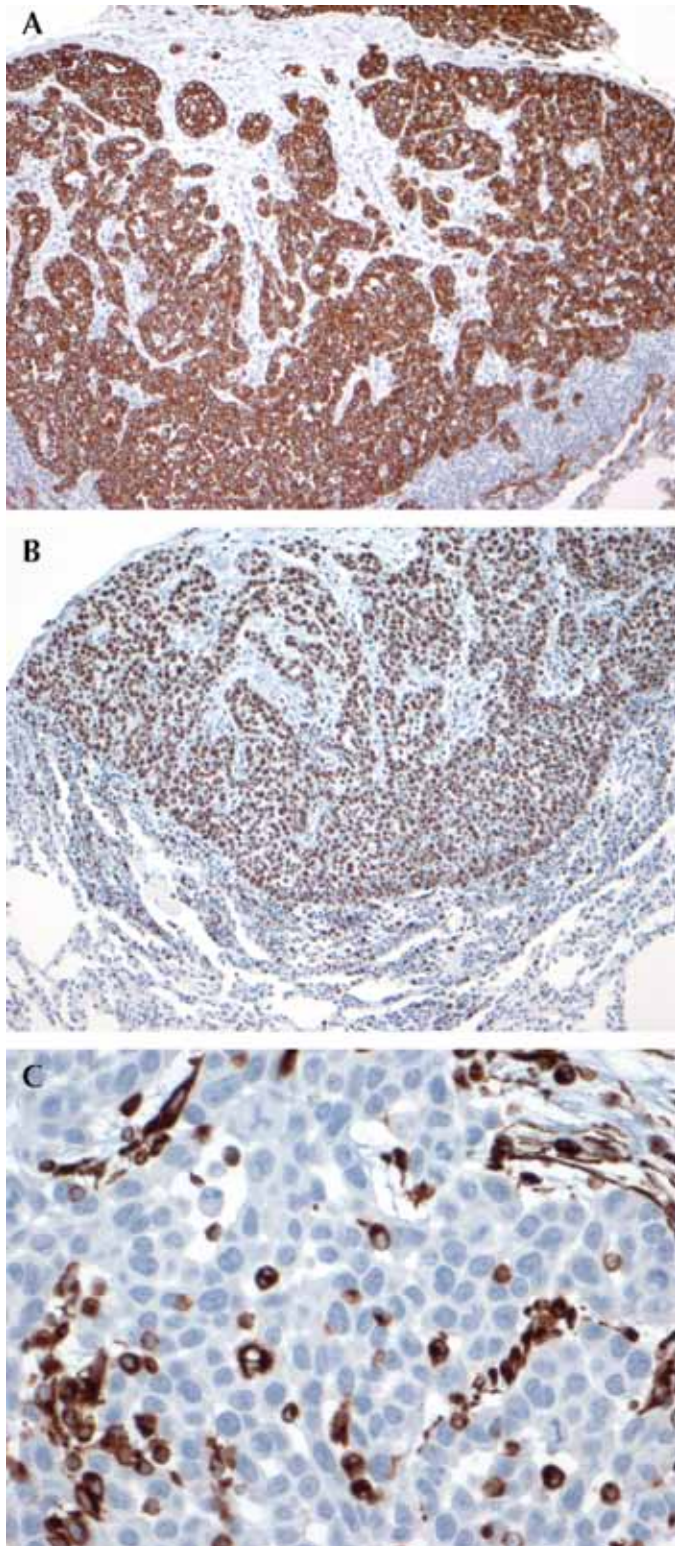


**Figure 5.** (A) Immunohistochemistry for keratin AE1/AE3 shows strong positive cytoplasmic staining in the tumor cells. Immunoperoxidase stain; magnification,  $\times 100$ . (B) Immunohistochemistry for the proliferation marker Ki67 is positive in 90% of the tumor cells. Immunoperoxidase stain; magnification,  $\times 100$ . (C) Immunohistochemistry for vimentin shows scattered tumor cell positivity. Immunoperoxidase stain; magnification,  $\times 400$ .

deterioration occurred rapidly, and some animals died with large pleural effusions.

This animal model is practical for research purposes for a number of reasons. First, 3- to 4-kg rabbits are relatively easy to work with and not prohibitively expensive to purchase or house. They develop consistently detectable pleural cancer within a reasonable time frame for research studies and are sufficiently large to accommodate the use of invasive and minimally invasive surgical and diagnostic procedures using standard surgical instrumentation. Second, successful pleural tumor development could be obtained after inoculation from freshly prepared tumor cell suspensions harvested directly from tumor-containing rabbits, ongoing cell cultures, or frozen tumor cells or tissue blocks. This characteristic allows flexibility in experimental design and costs. We believe that a key component to the success of this model is the use of mild pleural abrasion during thoracoscopy, thereby enabling localized tumor adherence and implantation. We suspect that other, less aggressive tumor lines may also be capable of successful adaptation to pleural cancer modeling according to these techniques. Although our approach used thoracoscopy and direct visualization during the procedure, this screening for tumors likely can also be accomplished in ways that will not require direct visualization, such as magnetic resonance imaging or computed tomography.

This study and our pleural cancer animal model both have several limitations. Because it uses a carcinoma cell line, our animal model cannot be applied to investigating progressive transformation in situ or the dysplastic and metaplastic changes occurring in primary pleural malignancy. However, this drawback is a limitation of all transplanted tumor models and not unique to this pleural model. From a practical standpoint, several animals developed large pleural effusions or rapidly deteriorated and died as tumors grew. Therefore, the timing of interventions in studies may be somewhat difficult to standardize. Some form of routine surveillance such as chest radiographs may be needed to monitor progression. Although they are considerably larger than previously described rodent models and can be used in a number of previously unavailable surgical and diagnostic investigations, rabbits are still much smaller than adult humans. Therefore extrapolation of certain treatment regimens that are highly depth-sensitive (including radiation and photo therapies) may still have limitations with this model. Conversely, the size advantage of rabbits over murine models may be offset by higher costs and lack of genetically engineered and knockout models in rabbits compared with mice, depending on the research application focus.<sup>13,16</sup> Murine pleural cancer models have been well described for these applications.<sup>5,7,9</sup> For future research by groups with specific research needs, altering various aspects of this animal model to meet specific needs may overcome some of these current limitations. Further, perhaps some of the techniques we described might be applicable in even larger animal models.

In conclusion, this report describes the first successful development of a method for consistently producing pleural cancer in a moderate-sized animal model. Several aspects of this model parallel the clinical features of patients with pleural cancers and likely will facilitate further investigations into the diagnosis and treatment of pleural cancers. We speculate that these methods may be adaptable to other tumor types and possibly other large animals to meet ongoing important needs in pleural cancer research.

## Acknowledgments

We gratefully acknowledge the contributions of Nevine Hanna, Andrew Duke, Reza Mina-Araghi, Chung Ho Sun, Hongrui Li, Lih-huei Liao, Teri Waite Kennedy, David Mukai, Jerry Wong, and Sabea Molloy for their technical assistance with this work. We also extend our gratitude to Dr John D Hazle (University of Texas, MD Anderson Cancer Center, Houston, Texas), who supplied us with the initial VX2 cancer cell line and cell maintenance protocol used for this model. This project was funded by Department of Defense (grant no. AF 9550-04-1-0101) and Philip Morris USA (grant no. 32598).

## References

1. **Bennett R, Maskell N.** 2005. Management of malignant pleural effusions. *Curr Opin Pulm Med* **11**:296–300.
2. **Goldberg SN, Gazelle GS, Compton CC, Mueller PR, McLoud TC.** 1996. Radio-frequency tissue ablation of VX2 tumor nodules in the rabbit lung. *Acad Radiol* **3**:929–935.
3. **Georges E, Breitburd F, Jibard N, Orth G.** 1985. Two Shope papillomavirus-associated VX2 carcinoma cell lines with different levels of keratinocyte differentiation and transplantability. *J Virol* **55**:246–250.
4. **Hughes RS.** 2005. Malignant pleural mesothelioma. *Am J Med Sci* **329**:29–44.
5. **Kane AB.** 2006. Animal models of malignant mesothelioma. *Inhal Toxicol* **18**:1001–1004.
6. **Kidd JG, Rous P.** 1940. A transplantable rabbit carcinoma originating in a virus induced papilloma and containing the virus in a masked or altered form. *J Exp Med* **71**:813–838.
7. **Martarelli D, Catalano A, Procopio A, Orecchia S, Libener R, Santoni G.** 2006. Characterization of human malignant mesothelioma cell lines orthotopically implanted in the pleural cavity of immunodeficient mice for their ability to grow and form metastasis. *BMC Cancer* **6**:130–136.
8. **Martinez-Moragon E, Aparicio J, Sanchis J, Menendez R, Cruz Rogado M, Sanchis F.** 1998. Malignant pleural effusion: prognostic factors for survival and response to chemical pleurodesis in a series of 120 cases. *Respiration* **65**:108–113.
9. **Matsumoki Y, Yano S, Goto H, Nakatali E, Wedge SR, Ryan AJ, Sone S.** 2006. ZD6474, an inhibitor of vascular endothelial growth factor receptor tyrosine kinase, inhibits growth of experimental lung metastasis and production of malignant pleural effusions in a non-small cell lung cancer model. **16**:15–26.
10. **Mountain CF.** 2000. The international system for staging lung cancer. *Semin Surg Oncol* **18**:106–115.
11. **Reeder LB.** 2001. Malignant pleural effusions. *Curr Treat Options Oncol* **2**:93–96.
12. **Rice TW, Blackstone EH.** 2002. Radical resections for T4 lung cancer. *Surg Clin North Am* **82**:573–587.
13. **Robinson C, van Bruggen I, Segal A, Dunham M, Sherwood A, Koentgen F, Robinson BW, Lake RA.** 2006. A novel SV40 TAG transgenic model of asbestos-induced mesothelioma: malignant transformation is dose-dependent. *Cancer Res* **66**:10786–10794.
14. **Rous P, Kidd JG, Smith WE.** 1952. Experiments on the cause of the rabbit carcinomas derived from virus-induced papillomas. II. Loss by the Vx2 carcinoma of the power to immunize hosts against the papilloma virus. *J Exp Med* **96**:129–174.
15. **Stathopoulos J, Antoniou D, Stathopoulos GP, Rigatos SK, Dimitroulis J, Koutandos J, Michalopoulou P, Athanasiades A, Veslemes M.** 2005. Mesothelioma: treatment and survival of a patient population and review of the literature. *Anticancer Res* **25**:3671–3676.
16. **Stathopoulos GT, Zhu Z, Everhart MB, Kalomenidis I, Lawson WE, Bilaceroglu S, Peterson TE, Mitchell D, Yull FE, Light RW, Blackwell TS.** 2006. Nuclear factor  $\kappa$ B affects tumor progression in a mouse model of malignant pleural effusion. *Am J Respir Cell Mol Biol* **34**:142–150.
17. **The American Thoracic Society and The European Respiratory Society.** 1997. Pretreatment evaluation of non-small-cell lung cancer. *Am J Respir Crit Care Med* **156**:320–332.
18. **Yano S, Herbst RS, Shinohara H, Knighton B, Bucana CD, Killion JJ, Wood J, Fidler JJ.** 2000. Treatment for malignant pleural effusion of human lung adenocarcinoma by inhibition of vascular endothelial growth factor receptor tyrosine kinase phosphorylation. *Clin Cancer Res* **6**:957–965.
19. **Zucali PA, Giaccone G.** 2006. Biology and management of malignant pleural mesothelioma. *Eur J Cancer* **42**:2706–2714.